Predicted Fusion Performance for DEMO Plasmas Using a BALDUR Code With Complete Predictive Pedestal Boundary Model

W. Buangam1), Y. Onsa1), B. Somjinda1), S. Sangaroon2), A. Wisitsorasak3), B. Chatthong4), J. Promping5), and T. Onjun1)
1) School of Manufacturing Systems and Mechanical Engineering, Sirindhorn International Institute of Technology, Thammasat University, Klongluang, Pathumthani, Thailand
2) Department of Physics, Mahasarakham University, Mahasarakham, Thailand
3) King Mongkut's University of Technology Thonburi, Bangkok, Thailand
4) Department of Physics, Faculty of Science, Prince of Songkla University, Songkla, Thailand
5) Thailand Institute of Nuclear Technology, Bangkok, Thailand

E-mail contact of main author: thawatchai@siit.tu.ac.th

Abstract. A simple model for predicting density of hydrogenic and impurity species at the top of the pedestal is developed and implemented in the BALDUR integrated predictive modeling code. In addition, a simple estimation of tritium flux generated from lithium blanket is developed based on the Monte Carlo code MCNP5 calculation. This suite of code is then used to carry out an evolution of plasma current, densities and temperature in DEMOs (designs proposed by China and India). In these simulations, a combination of NCLASS neoclassical transport and Multi-mode anomalous transport models is used to compute a core transport. There are 5 plasma species considered, including deuterium, tritium, helium, beryllium, and carbon. It is found that the temperatures at the center are in a good range for fusion reactions for both designs. However, the pedestal temperature is found to be lower than 3 keV, which is due to high density at the top of the pedestal. It is also found that the helium density is the highest and the carbon density is the lowest. In addition, the performance for India DEMO is almost double of that for China DEMO.

1. Introduction

The concept of magnetic confinement fusion has long been explored to address the feasibility of nuclear fusion energy. ITER [1] is an international collaborative effort with the objective of demonstrating the scientific and technological feasibility of nuclear fusion. The goal of ITER is to produce plasmas with a sufficiently high fusion energy density for a long enough time to achieve a sustained fusion burn. In addition, DEMO has been planned for explore the possibility of a fusion power plant. Producing a significant fusion reaction rate inside a tokamak requires the ability to heat and to contain high-temperature plasmas. Since the high confinement mode (H-mode) plasmas in tokamaks generally provide excellent energy confinement and have acceptable particle transport rates for impurity control, fusion experiments in ITER and DEMOs are designed to operate in the *H*-mode regime. It is widely known that there is a significant increase in the core pressure, from the L-mode discharge to the H-mode discharge. The significant enhancement in the plasma performance is the result of a transport barrier that forms at the edge of the plasma. This edge transport barrier (ETB) is usually referred as the "pedestal". Typically, the energy content in an H-mode discharge is approximately twice the energy contained in an L-mode discharge, for the plasma heated with the same input power.

Recently, several simulations had been carried out to investigate capability of several designs of DEMO reactors in terms of fusion performance based on different numerical calculations. However, the computational details in these simulations may differ and different assumptions may be assumed. The ultimate goal of the present work is to intensively investigate the performance of DEMO reactors by a self-consistent model. This, in turn, can provide insightful information and give feedbacks to the fusion research and development community.

In this work, a BALDUR integrated predictive modeling code [2] is used to simulate the time evolution of plasma temperature, density and current proles for two DEMO designs including the designs proposed by research teams from China[3] and India [4]. The chosen designs is based on available information of the reactors. A combination of MMM95 core transport model and NCLASS neoclassical transport is employed to describe the thermal transport, as well as the particle and impurity transport. The boundary conditions are calculated using the pedestal temperature based on the magnetic shear and flow shear stability width model combined with the ballooning mode instability pressure gradient limits and the pedestal density based on the line average density. In addition, crucial phenomena in tokamak plasmas, such as sawtooth oscillation, are considered. This suite of BALDUR code has been intensively validated against many plasma conditions from various tokamaks and compared with several modeling codes.

2. BALDUR integrarated predictive modeling code

The BALDUR integrated predictive modeling code is a multi-fluid transport code which solves time-dependent one-dimensional radial diffusion equations for plasma profiles.

2.1 Models for density at the top of pedestal

A boundary condition for the BALDUR code is set at t a top of the pedestal of the H-mode plasma. The width of the temperature pedestal Δ is assumed to be determined by a combination of magnetic and flow shear stabilization of drift modes,

$$\Delta = 2.42 \rho s^2 ,$$

where C_W is a constant, s is the magnetic shear and ρ is the ion gyro-radius at the inner edge of the steep gradient region of the pedestal. In the steep gradient region of the pedestal, the pressure gradient is assumed to be constant and to be limited by the ideal, short wavelength, MHD ballooning mode limit. This first stability ballooning mode limit can be approximated by

$$\alpha_c = 0.4s\left(1+\kappa_{95}^2\left(1+5\delta_{95}^2\right)\right),$$

where κ95 and δ95 are the elongation and triangularity at the 95% magnetic surface, respectively.

The pedestal pressure is taken to be the product of the pedestal width and the critical pressure gradient. The pedestal temperature T_{ped} can be written as [15]

$$T_{ped} = 1.89\left(\frac{B}{q^2}\right)^2\left(\frac{A_H}{R^2}\right)\left(\frac{\alpha_c}{n_{ped,19}}\right)^2 s^4 ,$$

where B is the toroidal magnetic field, q is the safety factor, A_{H} is the average hydrogenic ion mass in atomic mass units, R is the major radius and $n_{\mathrm{ped,19}}$ is the electron density at the top of the pedestal in units of 10^{19} m^{-3}.

The experimental line average density and pedestal density of deuterium and carbon are obtained from 15 JET H-mode discharges in International Profile Database, which shown in Figs. 1 and 2. It can be seen that both parameters correlate with each other very well. Statistically, it is found that the correlation coefficient (R^2) between line average density and pedestal density for deuterium and carbon are 0.96 and 0.88, respectively. Thus, in this work, the following expressions are used for estimating the density of all hydrogenic and impurity species:

$$n_{\mathrm{ped,hyd}} = 0.76 n_{\mathrm{l,hyd}}$$

$$n_{\mathrm{ped,imp}} = 0.77 n_{\mathrm{l,imp}} \, .$$

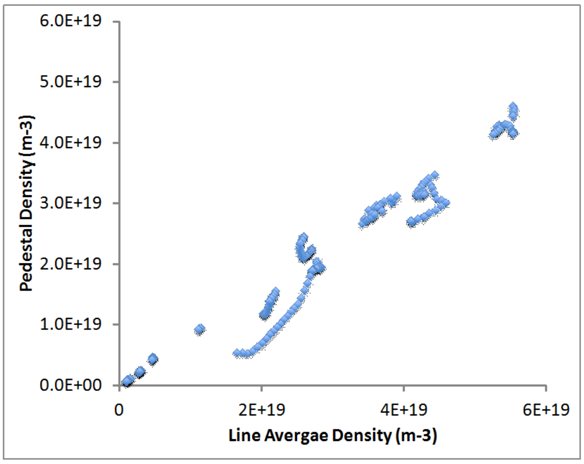

Fig. 1: The line average density, plotted on the horizontal axis, is compared with pedestal deuterium density, plotted on the vertical axis, for 276 experimental data points from the International Pedestal Database.

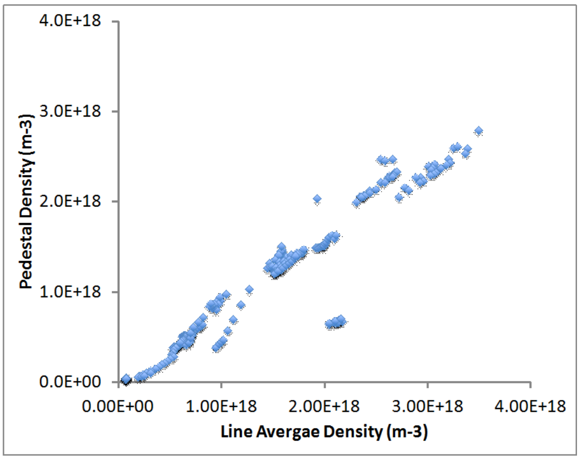

Fig. 2: The line average density, plotted on the horizontal axis, is compared with pedestal carbon density, plotted on the vertical axis, for 276 experimental data points from the International Pedestal Database.

2.2 Model for tritium breeding

The production of tritium from the lithium self-cooled blanket with a vanadium alloy structure (Li/V) is obtained using the Monte Carlo N-Particle transport code (MCNP). The mock-up blanket is set up with five layers of lithium, reflector, shielding and the structure. The different types of liquid lithium have been considered including natural lithium, FLiBe and LiPb. The obtained tritium production rate per source neutron shows in figure 3(a) while the ratio of tritium to neutron shows in figure 3(b).

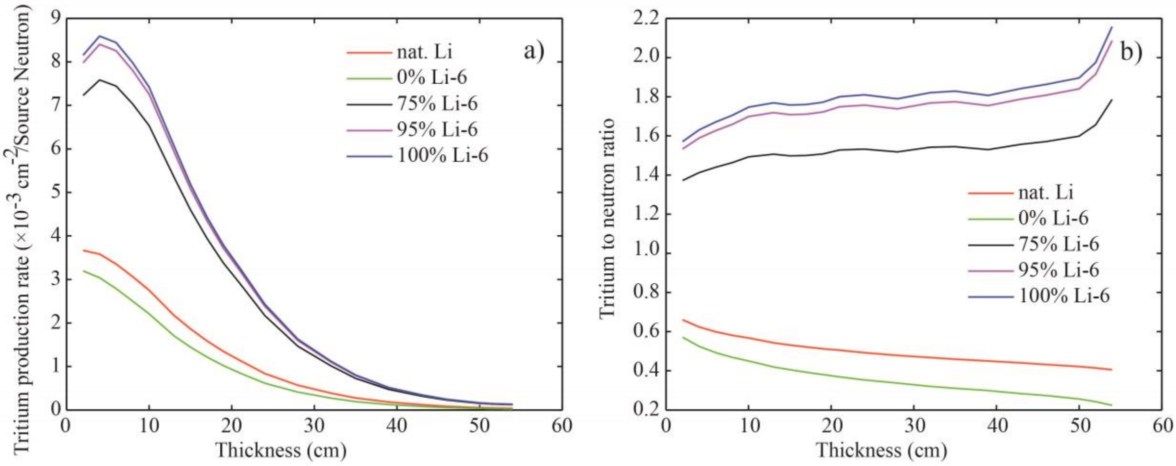

Fig. 3: (a) Tritium production rate per source neutron and (b) tritium to neutron ratio in breeder zone of different ^{6}Li concentrations in LiPb breeding material composition

It is found that the tritium production increased with the increasing percent ^{6}Li enrichment and decreased due to the increasing breeder layer. The high ^{6}Li concentration in the LiPb produced the highest tritium to neutron ratio. With 75 percent ^{6}Li enrichment in the LiPb, the ratios of tritium production to each neutron in the local breeding layer were about 1.528.

2.3 Plasma transport model

In this work, the core transport code can be described by a linear combination of neoclassical and anomalous transport.

2.3.1 Anomalous transport

The anomalous transport (MMM95 model) is a linear combination of theory-based transport models which consists of the Weiland model for the ion temperature gradient (ITG) and trapped electron modes (TEM), the Guzdar–Drake model for drift-resistive ballooning modes, as well as a smaller contribution from kinetic ballooning modes. The Weiland model for drift modes such as ITG and TEM modes usually provides the largest contribution to the MMM95 transport model in most of the plasma core. The Weiland model is derived by linearizing the fluid equations, with magnetic drifts for each plasma species. Eigenvalues and eigenvectors computed from these fluid equations are then used to compute a quasilinear approximation for the thermal and particle transport fluxes. The Weiland model includes many different physical phenomena such as effects of trapped electrons, $T_i \neq T_e$, impurities, fast ions, and finite β. The resistive ballooning model in MMM95 transport model is based on the 1993 *ExB* drift-resistive ballooning mode model by Guzdar–Drake, in which the transport is proportional to the pressure gradient and collisionality. The contribution from the resistive ballooning model usually dominates the transport near the plasma edge. Finally, the kinetic ballooning model is a semi-empirical model, which usually provides a small contribution to the total diffusivity throughout the plasma, except near the magnetic axis. However, for the ITER case in this work, it is surprisingly found that the contribution from the kinetic ballooning mode plays quite a significant role in the region near the plasma core up to a radius of 1.0 m. This will be discussed in Section 3. This model is an approximation to the first ballooning mode stability limit.

$$\chi_i = 0.8\chi_{i,ITG\&TEM} + \chi_{i,RB} + 0.65\chi_{i,KB}$$
$$\chi_e = 0.8\chi_{e,ITG\&TEM} + \chi_{e,RB} + 0.65\chi_{e,KB}$$
$$D_H = 0.8 D_{H,ITG\&TEM} + D_{H,RB} + D_{H,KB}$$
$$D_Z = 0.8 D_{Z,ITG\&TEM} + D_{Z,RB} + D_{Z,KB}$$

All the anomalous transport contributions to the MMM95 transport model are multiplied by κ^{-4}, since the models were originally derived for circular plasmas.

2.3.2 NCLASS Module

The NCLASS module calculates the neoclassical transport properties of multi-species axisymmetric plasma of arbitrary aspect ratio, geometry and collisionality. The neoclassical effects refer to the flows of Coulomb collisions between particles drifting in nonuniform magnetic and electric fields. This module determines a multi-fluid model for the parallel and radial force balance equations from which the neoclassical bootstrap current, parallel electrical resistivity, impurity and fuel ion radial particle transport, ion radial thermal transport and plasma poloidal rotation. It is designed to be called from a transport code that provides the plasma density and temperature profiles.

3. Results and discussion

All simulations in this work are carried out based on a standard type-I ELMy H-mode scenario of DEMO designs using the BALDUR integrated predictive modelling code. Some design engineering parameters used in this work can be seen in Table 1. In addition, the duration of each DEMO simulation running time is set at 1000 s, of which the plasma current and density are slowly ramped up to the designated values within the first 100 s. It is observed in all simulations that the plasma reaches a stationary state quickly after the plasma current reaches the maximum value. In the stationary state, the plasma still varies with some degrees of fluctuations due to plasma instability, i.e. sawtooth oscillation. There are 5 plasma species considered, including deuterium and tritium as working gas, and helium, beryllium, and carbon as impurity.

Table 1: List of engineering parameters for each DEMO design

Parameters	China	India
R (m)	7.2	7.7
a (m)	2.1	2.6
$I_p (MA)$	14.8	17.8
$B_T (T)$	6.86	6
κ	1.85	1.7
δ	0.45	0.33
$Plasma\ Volume\ \ (m^3)$	1056	1647
$n_{e,l} (10^{20} m^{-3})$	1.5	0.77
$P_{aux} (MW)$	74	110

The plasma temperature and density profiles for China and India DEMOs at 1,000 sec are shown in figure 1. Note that the simulations with 2 different gas recycling rate (r_{cly} = 0.0 and r_{cly} = 0.5). This can be seen, which illustrates the simulation results for ion temperature (T_i), electron temperature (T_e), ion density (n_i) and electron density (n_e) as a function of normalized minor radius at 1000 s. In addition, the values for plasma parameters (ion temperature, electron temperature, deuterium density, tritium density, helium density, beryllium density, and carbon density) at the center and pedestal at 1,000 sec are summarized in Table 2 for each DEMO design. It can be seen that the temperatures at the center are in a good range for fusion reactions. However, it is worth to mention that the pedestal temperature is lower than 3 keV, which is due to high density at the top of the pedestal. It is also worth to mention about the impurity density. It can be seen that the helium density is the highest and the carbon density is the lowest.

Table 2: Summary for plasma parameters at the center and pedestal at 1,000 sec for each DEMO design

Region	**Parameters**	**China**		**India**	
		r_{cly}=0.0	r_{cly}=0.5	r_{cly}=0.0	r_{cly}=0.5
Center	$T_{i,0}$ [keV]	30.9	31.7	27.0	27.0
	$T_{e,0}$ [keV]	32.5	32.6	31.2	31.6
	$n_{D,0}$ [10^{19} m-3]	3.7	3.7	4.0	4.0
	$n_{T,0}$ [10^{19} m-3]	2.7	2.6	3.5	3.4
	$n_{He,0}$ [10^{19} m-3]	1.1	1.1	1.3	1.3
	$N_{Be,0}$ [10^{17} m-3]	5.4	5.4	4.9	5.0
	$n_{C,0}$ [10^{15} m-3]	7.1	7.0	8.0	8.0
Pedestal	$T_{i,ped}$ [keV]	2.6	2.6	2.0	2.0
	$T_{e.ped}$ [keV]	2.6	2.6	2.0	2.0
	$n_{D,ped}$ [10^{19} m-3]	3.2	3.3	3.1	3.1
	$n_{T,ped}$ [10^{19} m-3]	2.5	2.4	2.8	2.7

	$n_{He,ped}$ [10^{18} m-3]	7.6	7.6	8.7	8.8
	$N_{Be,ped}$ [10^{17} m-3]	4.4	4.4	3.8	3.8
	$n_{C,ped}$ [10^{15} m-3]	7.7	7.7	7.7	7.7

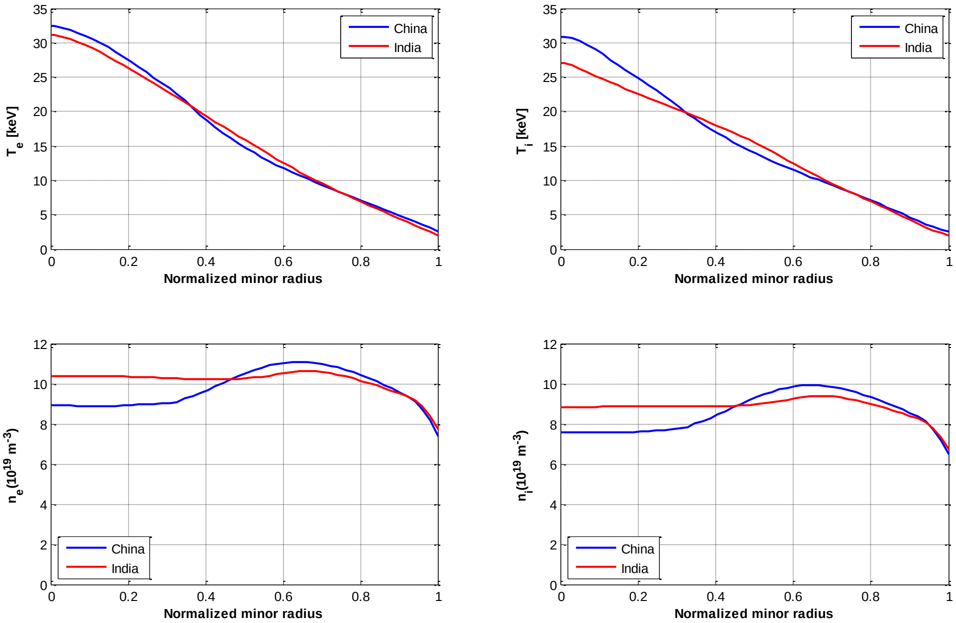

Fig.1: The plasma profiles for China and India DEMOs at 1,000 sec with gas recycling rate (r_{cly} = 0.0) are plotted as a function of normalized minor radius.

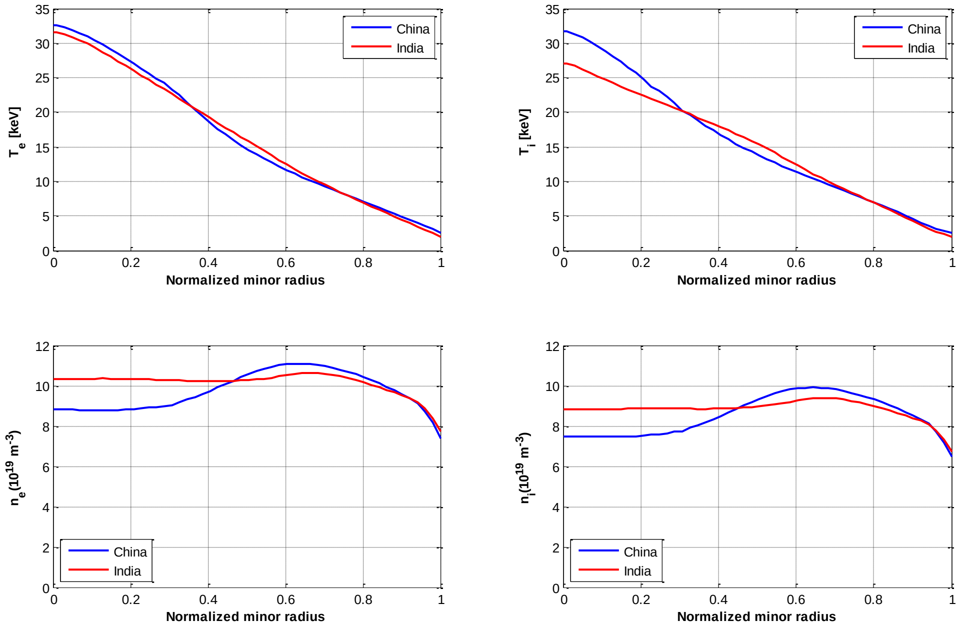

Fig.2: The plasma temperature and density profiles for China and India DEMOs at 1,000 sec with gas recycling rate (r_{cly} = 0.5) are plotted as a function of normalized minor radius.

The plasma performance for China and India DEMOs are obtained from those simulations and summarized in Table 3. It can be seen that the performance for India DEMO is almost double of that for China DEMO.

Table 3: Summary for plasma performance for each DEMO design

Parameters	**China**		**India**	
	r_{cly}=0.0	r_{cly}=0.5	r_{cly}=0.0	r_{cly}=0.5
P_{alpha} [MW]	98	93	180	180
P_{rad} [MW]	20	20	34.1	34.2
τ_E [sec]	2.5	2.5	2.4	2.5

4. Conclusion

BALDUR integrated predictive modeling code is used to carry out an evolution of plasma current, densities and temperature in DEMOs (designs proposed by China and India). It is found that the temperatures at the center are in a good range for fusion reactions for both designs. However, the pedestal temperature is found to be lower than 3 keV, which is due to high density at the top of the pedestal. It is also found that the helium density is the highest and the carbon density is the lowest. In addition, the performance for India DEMO is almost double of that for China DEMO.

Acknowledgements

This work is part of a collaborative research project under the Center of Plasma and Nuclear Fusion Technology (CPaF).

Reference

[1]C. E. Singer, *et al.*Comput. Phys. Commun. **49** (1988) 399

[2] Feng K., Zhang G., Zheng G., Zhao Z., Yuan T., Li Z., Sheng G. and Pan C. 2009 Fusion Eng. Des. 84 2109–13

[3] Srinivasan R. et al 2008 Fusion Eng. Des. 83 889–92